Lowland Technology International 2017; 19 (2): 87-98
International Association of Lowland Technology (IALT): ISSN 1344-9656

Research paper

Laterally loaded piles in multi-layered soils

M. Cao

ARTICLE INFORMATION

Article history:

Received: 04 April, 2017
Received in revised form: 02 August, 2017
Accepted: 04 August, 2017
Publish on: 08 September, 2017

Keywords:

Fictitious pile
Lateral load
Analytical solution
Layered soils
Transfer matrix method

ABSTRACT

The paper presents a rigorous analytical method, using the theory of the transfer matrix method for calculating the laterally loaded piles in multi-layered soils. Following the technique proposed by Muki and Sternberg, the problem is decomposed into extended layered soils and a fictitious pile characterized respectively by Young's moduli of the layered soils and those of the differences between the piles and the layered soils. The unknown bending moments along the fictitious pile are determined by solving a Fredholm integral equation of the second kind, which imposes the compatibility condition that the lateral displacements of the fictitious pile are equal to those corresponding to the centroidal axe of the extended layered soils. The pile lateral displacement and slope distributions can be calculated based on the determined fictitious pile bending moment distribution. Selected results from parametrical studies are presented to confirm the validity of the proposed approach and to portray the influence of the governing parameters on the pile bending moment, displacement and slope distributions.

1. Introduction

Piles are widely used to as the foundation in soft deposit to bearing vertical load from super-structure, to prevent subsidence due to groundwater pumping (Xu et al., 2016), and to support laterally loaded structures, such as high-rise buildings, bridges, offshore platforms, nearby geotechnical constructions (Wang et al., 2013, 2014; Wu et al., 2015d; Zhang et al., 2015; Shen et al., 2013b, d), deep excavation or tunnel construction etc. (Shen et al., 2014, 2016; Wu et al., 2015a-c; Wu et al., 2016). These buildings have to resist sever lateral loads caused by wind, earthquake, wind, waves, etc.. For a 100-m-tall building in Hong Kong, a typical design ultimate horizontal load may be as high as 2000 kN (Ng and Zhang, 2001). Therefore, much work has been done on analyzing the load-deformation behavior of piles subjected to lateral loads by many researchers, including the p-y method (Matlock, 1970; Reese and Welch, 1975; and Reese et al., 1974), the elastic continuum method (Poulos, 1971; Banerjee and Davis, 1978; Poulos and Davis, 1980; and Shen et al., 2013a, c, 2017), finite element method (Randolph, 1981; Trochanis et al., 1991; and Shen and Xu 2011), and elastic subgrade reaction method (Hetenyi, 1946; Reese and Matlock, 1956; and Davisson and Gill, 1963).

All the above mentioned methods, however, have limitations. For example, the finite element method is capable of modeling soil non-linearity, soil continuity and pile-soil interface behavior. However, the finite element method cannot be used in the routine design because of the effort required in modeling and computation. Hence, three main approaches, the p-y method, the elastic subgrade reaction method and the elastic continuum method are often used for analysis of laterally loaded piles. The soil resistance is modeled with discontinuous springs in the subgrade reaction method. The p-y method exhibits limitations similar to the subgrade reaction

Assistant Professor, Institute of Science and Technology, Shanghai Open University, Shanghai 200433, CHINA,
mingcaoxh@hotmail.com, caom@sou.edu.cn
Note: Discussion on this paper is open until April 2018

method except that soil resistance is considered to be a non-linear function of pile displacement. The elastic continuum method, taking into account the continuity of the soil mass, is a more accurate solution considering the pile as a very thin rectangular strip and using Mindlin's equation (1936) for a point load in the interior of an elastic half-space to obtain the deflections at various points along the pile due to a force applied at one level.

Most of the elastic solutions consider piles embedded in a homogeneous soil system. Since in most applications, piles are installed in layered soils, a method which considers the piles in a layered soils is an important part of the analysis of pile foundations. Pise (1982) employed the Mindlin's equation to study the effect of soil layering on the behavior of laterally loaded piles. The location of the maximum bending moment was not evaluated. Because Mindlin's solution is valid only for homogeneous continuums, this analysis is strictly not capable to laterally loaded piles in layered soils. Because Mindlin's solution is used, the finite difference method (Yang et al., 2002; and Yang and Liang, 2006) is only appropriate for laterally loaded piles in a two-layered soil system and it cannot be used for a more general situation, such as piles in a multi-layered soil system. In addition, analyses of a laterally loaded piles installed in multi-layered soils were done by assuming mathematical forms for the displacement field in the soil and minimizing potential energy for the pile-soil system (Basu and Salgado, 2007, 2010; Basu et al., 2009).

In this paper, the laterally loaded piles in multi-layered soils are reexamined and the above mentioned limitations for conventional calculation of the pile-soil interaction may be removed by using the fictitious pile method originally proposed by Muki and Sternberg (1970), which have been used for analysing vertically loaded piles (Cao and Chen, 2008, 2011, 2012; Cao et al., 2007). The analysis is thus similar in principle to analyses previously made for a laterally loaded bar which is partially embedded in a three-dimensional elastic half space (Pak, 1989). The layered soils are calculated by the theory of the transfer matrix, which is an extension to Muki (1960) and Sneddon (1992) solutions for multi-layered soils. The bending moment, the real pile lateral displacement as well as the pile slope over the length of the pile can be readily determined. The results obtained are confirmed via comparisons with the available results. Selected results from parametrical studies are presented to portray the influence of the governing parameters on the pile bending moment, displacement and slope distributions.

2. Mathematical formulation

In this section, a mathematical formulation is presented for the investigation of the behavior of a single laterally loaded pile embedded in layered soils. As shown in **Fig. 1,** let $\{0,x,y,z\}$ be a rectangular Cartesian coordinate frame spanning the semi-infinite elastic continuum with elastic properties of the layered soil medium B. For the purpose of explanation, there are two-layered elastic soils. Three or more layers of foundation can by analogy. The upper soil layer is of thickness H_1, with Young's modulus E_{s1}, Poisson's ratio μ_{s1}, overlying an infinite lower layer of modulus E_{s2}, Poisson's ratio μ_{s2}

A circular pile of radius a, length L, Yung's modulus E_p, and circular cross-sectional region Π_z $(0<z<L)$ is embedded in layered soils. The pile is denoted by B' (**Fig. 1(a)**).

.

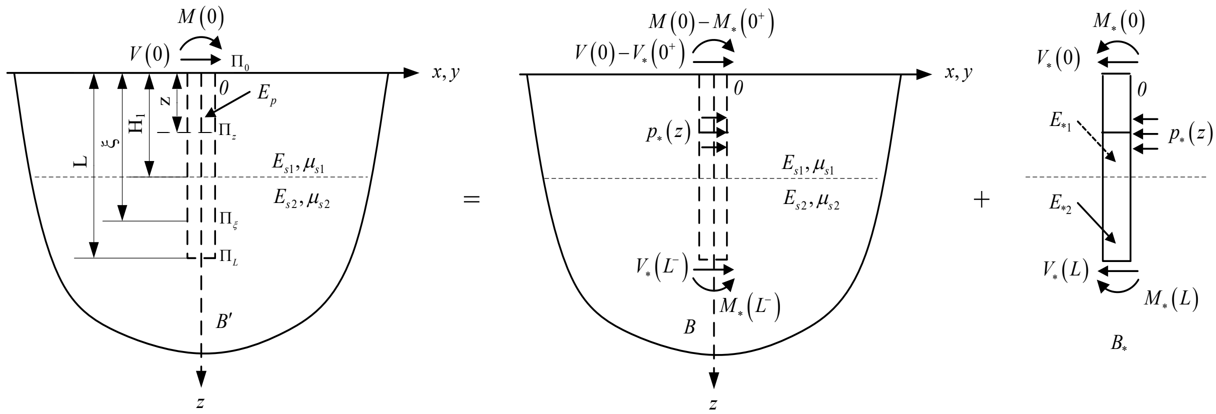

(a) Laterally loaded pile embedded in semi-infinite soil (b) Extended layered soils (c) Fictitious pile

Fig. 1. Laterally loaded pile embedded in elastic semi-infinite layered soils.

As in the treatment by Muki and Sternberg (1970) of this class of problems, the embedding soil medium is extended throughout the half space and the fictitious pile B_* is introduced throughout their original location to account for the presence of the embedded pile (**Fig. 1(c)**). The Young's modulus E_{*i} of the fictitious pile is equal to the differences between that of the real pile and the respective Young's moduli of extended layered soils, i.e.

$$E_{*i} = E_p - E_{si}, \ (i = 1, 2) \quad [1]$$

where E_{si} is the Young's modulus of the soil layer i, and the subscript $i = 1$ or 2 denotes the soil layer number.

The pile is loaded with a combination of lateral shear force $V(0)$ and a moment $M(0)$ at its head (**Fig. 1(a)**). The extended layered soils as shown in **Fig. 1(b)** are treated a three-dimensional elastic continuum with elastic properties of the layered soils. Following the technique of Pak (1989), the fictitious reinforcement B_* is regarded as one-dimensional elastic structure. The bending moment - displacement relation B_* can be expressed in the forms

$$E_{*1} I \frac{d^2 u_*(z)}{dz^2} = M_*(z), \ 0 \le z < H_1 \quad [2a]$$

$$E_{*2} I \frac{d^2 u_*(z)}{dz^2} = M_*(z), \ H_1 \le z \le L \quad [2b]$$

and the equilibrium equations

$$\frac{dM_*(z)}{dz} = V_*(z) \quad [3]$$

$$\frac{dV_*(z)}{dz} = -p_*(z) \quad [4]$$

where $u_*(z)$, $M_*(z)$ and $V_*(z)$ =the lateral displacement, the bending moment and the shear force of the fictitious pile at depth z, respectively; $p_*(z)$ =the distributed normal force per unit length exerted by B on B_*. $E_{*i}I$ =the bending rigidity of the fictitious pile.

The loads from the pile to its embedding medium through concentrated bond force are direct load transfer clarified by Muki and Sternberg (1968). Treating the circumferential surface of the fictitious pile B_* as frictionless, the external forces acting on B_* are composed of the following items: (1) $V_*(0)$, the resultant shear force at the top of B_* after a direct shear transfer; (2) $M_*(0)$, the resultant bending moment at the top of B_* after a direct moment transfer; (3) $V_*(L)$, the resultant shear force at the bottom end of B_*; (4) $M_*(L)$, the resultant bending moment at the bottom of B_*; and (5) $p_*(z)$, the distributed normal force per unit length exerted by B on B_*. By the law of action and reaction, the forgoing forces acting on the extended layered soils B are: (1) $V(0) - V_*(0^+)$, the direct shear transfer to the extended layered soils from the fictitious pile at the cross-section Π_0; (2) $M(0) - M_*(0^+)$, the direct moment transfer to the extended layered soils from the fictitious pile at the cross-section Π_0; (3) $V_*(L)$, the shear transfer from the fictitious pile; (4) $M_*(L)$, the moment transfer from the fictitious pile; and (5) $p_*(z)$, the distributed normal force per unit length at the cross-section Π_z. As in the treatment by Pak (1989), if the assumption of small cross-sectional rotation of the pile is made, the direct moment transfers at the pile ends are negligible.

$$M_*(L) = 0 \quad [5]$$

and

$$M(0) - M_*(0^+) = 0 \quad [6]$$

The compatibility condition requires that the lateral displacement of the fictitious pile and the extended soil layers be equal along the z-axis of over the length of the pile caused by the system of interactive forces. This condition leads to the following relationship

$$u_*(z) = \left[V(0) - V_*(0^+)\right]\bar{u}_x(z,0) + V_*(L)\bar{u}_x(z,L) + \int_0^L p_*(\xi)\bar{u}_x(z,\xi)d\xi, \ 0 \le z \le L \quad [7]$$

where $\bar{u}_x(z,\xi)$ =influence displacement function which represents the displacement of the extended layered soils at the depth z along the axis of the real pile B' due to a circular load over the cross-section Π_ξ, acting in the positive x-direction, the resultant applied force having unit magnitude. This influence function may be obtained by the theory of the transfer matrix-bottom rigidity for layered soils which will be expressed later. Substituting Eq. [4] into Eq. [7] leads to

$$u_*(z) = \left[V(0) - V_*(0^+)\right]\bar{u}_x(z,0) + V_*(L)\bar{u}_x(z,L) - \int_0^L \frac{dV_*(\xi)}{d\xi}\bar{u}_x(z,\xi)\,d\xi, \ 0 \le z \le L \quad [8]$$

Eq. [8] represents the primary governing equation for the pile-layered soils interaction problem considered. With the aid of Eqs. [3, 5 and 6] and proper account of the discontinuity of the integrand during an integration by parts, Eq. [8] can be further reduced to a Fredholm equation of the second kind:

$$u_*(z)=V(0)\bar{u}_x(z,0)-M(0)\frac{\partial\bar{u}_x(z,0)}{\partial\xi}-M_*(z)\frac{\partial\bar{u}_x(z,\xi)}{\partial\xi}\Big|_{z^-}^{z^+}$$
$$-\int_0^L M_*(\xi)\frac{\partial^2\bar{u}_x}{\partial\xi^2}(z,\xi)d\xi,\quad 0\le z\le L \qquad [9]$$

Eq. [10] shows a horizontal circular load of unit intensity over the cross-section of radius *a* in elastic layered soils.

$$P=\frac{1}{2\pi a\sqrt{a^2-r^2}} \qquad [10]$$

With the aid of Eq. [10], the influence shear stress function $\tau_{zx}(z,z^+)$, which is defined as the shear stress of the extended layered soils at the depth z due to a horizontal circular load at the depth z^+, the resultant applied force having unit magnitude, has the following property

$$\tau_{zx}(z,z^+)-\tau_{zx}(z,z^-)=-\frac{1}{2A} \qquad [11]$$

where A is the area of the laterally loaded pile embedded in layered soils. According to the Generalized Hooke's Law, this influence function can be expressed as

$$\gamma_{zx}(z,z^+)-\gamma_{zx}(z,z^-)=\frac{1}{G_{si}}\left[\tau_{zx}(z,z^+)-\tau_{zx}(z,z^-)\right]$$
$$=-\frac{1}{2G_{si}A},(i=1,2) \qquad [12]$$

where $\gamma_{zx}(z,z^+)$ =influence shear strain function which represents the shear strain of the extended layered soils at the depth z due to a circular load at the depth z^+, acting in the positive *x*-direction, the resultant applied force having unit magnitude, and G_{si} =the shear modulus of the soil layer i.

This condition leads to (Cao, 2017)

$$\frac{\partial\bar{u}_x(z,z^+)}{\partial\xi}-\frac{\partial\bar{u}_x(z,z^-)}{\partial\xi}=-\frac{1}{2G_{si}A},\ (i=1,2) \qquad [13]$$

Substituting Eq. [13] into Eq. [9] yields

$$u_*(z)=V(0)\bar{u}_x(z,0)-M(0)\frac{\partial\bar{u}_x(z,0)}{\partial\xi}+\frac{M_*(z)}{2G_{si}A}$$
$$-\int_0^L M_*(\xi)\frac{\partial^2\bar{u}_x}{\partial\xi^2}(z,\xi)d\xi,\quad 0\le z\le L \qquad [14]$$

Eq. [14] can be simplified as

$$u_*(z)=-\int_0^L g_i(z,\xi)M_*(\xi)d\xi$$
$$+u_*(0)\left(1-\frac{z}{L}\right)+u_*(L)\left(\frac{z}{L}\right),\quad (i=1,2) \qquad [15]$$

where

$$g_1(z,\xi)=\frac{1}{E_{*1}I}\begin{Bmatrix}\left(1-\frac{\xi}{L}\right)z, & z<\xi\\ \left(1-\frac{z}{L}\right)\xi, & z>\xi\end{Bmatrix},\ 0\le z<H_1 \qquad [16a]$$

$$g_2(z,\xi)=\frac{1}{E_{*2}I}\begin{Bmatrix}\left(1-\frac{\xi}{L}\right)z, & z<\xi\\ \left(1-\frac{z}{L}\right)\xi, & z>\xi\end{Bmatrix},\ H_1<z\le L \qquad [16b]$$

For the analysis in dimensionless form the following dimensionless parameters are introduced

$$\bar{z}=\frac{z}{a}\ ,\ \ \bar{\xi}=\frac{\xi}{a}\ ,\ \ \bar{L}=\frac{L}{a}\ ,\ \ \bar{E}_i=\frac{E_p}{E_{si}}\ ,\ \ \kappa_i=\frac{8}{(1+\mu_{si})(\bar{E}_i-1)}\ ,$$
$$\bar{M}(0)=\frac{M(0)}{4\pi G_{si}a^3}\ ,\ \ \bar{M}=\frac{M_*}{4\pi G_{si}a^3}\ ,\ \ \bar{u}=\frac{u_*}{a}\ ,\ \ \bar{V}(0)=\frac{V(0)}{4\pi G_{si}a^2}\ ,$$
$$\bar{V}=\frac{V_*}{4\pi G_{si}a^2}\ ,\ (i=1,2)$$

With the aid of these parameters, the relevant second kind Fredholm integral equation that furnishes the unknown function $\bar{M}(\bar{z})$ and the top and bottom displacements of the fictitious pile B_* in extended layered soils can be expressed as the following form

$$B(\bar{z})\bar{u}(0)+C(\bar{z})\bar{u}(\bar{L})+\int_0^{\bar{H}_1}K_1(\bar{z},\bar{\xi})\bar{M}(\bar{\xi})d\bar{\xi}-2\bar{M}(\bar{z})$$
$$+\int_{\bar{H}_1}^{\bar{L}}K_2(\bar{z},\bar{\xi})\bar{M}(\bar{\xi})d\bar{\xi}$$
$$=\bar{V}(0)\bar{U}(\bar{z},0)-\bar{M}(0)\frac{\partial\bar{U}(\bar{z},0)}{\partial\bar{\xi}},0\le\bar{z}<\bar{H}_1,\bar{H}_1<\bar{z}\le\bar{L} \qquad [17]$$

where

$$B(\bar{z})=\left(1-\frac{\bar{z}}{\bar{L}}\right),\ C(\bar{z})=\frac{\bar{z}}{\bar{L}},\ \bar{U}(\bar{z},\bar{\xi})=4\pi G_{si}a\bar{u}(z,\xi),$$

$$\bar{g}_1(\bar{z},\bar{\xi}) = \begin{Bmatrix} \left(1-\dfrac{\bar{\xi}}{\bar{L}}\right)\bar{z}, & \bar{z}<\bar{\xi} \\ \left(1-\dfrac{\bar{z}}{\bar{L}}\right)\bar{\xi}, & \bar{z}>\bar{\xi} \end{Bmatrix},\ 0 \le z < H_1,$$

$$\bar{g}_2(\bar{z},\bar{\xi}) = \begin{Bmatrix} \left(1-\dfrac{\bar{\xi}}{\bar{L}}\right)\bar{z}, & \bar{z}<\bar{\xi} \\ \left(1-\dfrac{\bar{z}}{\bar{L}}\right)\bar{\xi}, & \bar{z}>\bar{\xi} \end{Bmatrix},\ H_1 < z \le L,$$

$$K_i(\bar{z},\bar{\xi}) = \sum_{i=1}^{2}\left[\frac{\partial^2 \bar{U}_i}{\partial \xi^2}(\bar{z},\bar{\xi}) - \kappa_i \bar{g}_i(\bar{z},\bar{\xi})\right],$$

$$\kappa_i = \frac{8}{(1+\mu_{si})(E_p/E_{si}-1)},\ (i=1,2)$$

Once $\bar{M}(\bar{z})$ has been found, the solution for the lateral displacement $\bar{u}(\bar{z})$ of the fictitious pile in the extended layered soils can be expressed as

$$\bar{u}(\bar{z}) = -\int_0^{\bar{L}} \kappa_i \bar{g}(\bar{z},\bar{\xi})\bar{M}(\bar{\xi})d\bar{\xi} + \bar{u}(0)\left(1-\frac{\bar{z}}{\bar{L}}\right) + \bar{u}(\bar{L})\left(\frac{\bar{z}}{\bar{L}}\right),\ (i=1,2) \qquad [18]$$

The differential equation of $\bar{u}(\bar{z})$ is obtained as

$$\bar{\theta}(\bar{z}) = -\int_0^{\bar{L}} \kappa_i H(\bar{z},\bar{\xi})\bar{M}(\bar{\xi})d\bar{\xi} + \frac{1}{\bar{L}}\left[\bar{u}(\bar{L}) - \bar{u}(0)\right],\ (i=1,2) \qquad [19]$$

where $\bar{\theta}(\bar{z})$ =the slope of the fictitious pile at depth z and

$$H(\bar{z},\bar{\xi}) = \begin{Bmatrix} 1-\dfrac{\bar{\xi}}{\bar{L}}, & \bar{z}<\bar{\xi} \\ -\dfrac{\bar{\xi}}{\bar{L}}, & \bar{z}>\bar{\xi} \end{Bmatrix}$$

3. Solution for influence displacement function in layered soils

To determine the influence displacement function, it is convenient to employ the transfer matrix method (Bufler, 1971; Bahar, 1972; and Ai et al., 2002). The influence function can be expressed as

$$\bar{u}(z,\xi) = \frac{1}{2}\int_0^\infty \zeta\left[\tilde{\Psi}_{11}(\zeta,z,\xi)J_2(\zeta r) + \tilde{\Psi}_{21}(\zeta,z,\xi)J_0(\zeta r)\right]d\zeta \qquad [20]$$

where $J_2(\zeta r)$ and $J_0(\zeta r)$ are Bessel functions of orders 2 and 0 respectively.

$$\tilde{\Psi}(\zeta,z,\xi) = \left[\tilde{S}_1^2(\zeta,z,\xi), \tilde{S}_2^0(\zeta,z,\xi), \tilde{w}^1(\zeta,z,\xi), \tilde{T}_1^2(\zeta,z,\xi), \tilde{T}_2^0(\zeta,z,\xi), \tilde{\sigma}_z^1(\zeta,z,\xi)\right]^T$$

$$\tilde{\Psi}(\zeta,0,\xi) = \left[\tilde{S}_1^2(\zeta,0,\xi), \tilde{S}_2^0(\zeta,0,\xi), \tilde{w}^1(\zeta,0,\xi), \tilde{T}_1^2(\zeta,0,\xi), \tilde{T}_2^0(\zeta,0,\xi), \tilde{\sigma}_z^1(\zeta,0,\xi)\right]^T$$

where $\tilde{S}_1^2(\zeta,z,\xi)$, $\tilde{S}_2^0(\zeta,z,\xi)$, $\tilde{w}^1(\zeta,z,\xi)$, $\tilde{T}_1^2(\zeta,z,\xi)$, $\tilde{T}_2^0(\zeta,z,\xi)$ and $\tilde{\sigma}_z^1(\zeta,z,\xi)$ stand for the Hankel transforms of $S_1^2(\zeta,z,\xi)$, $S_2^0(\zeta,z,\xi)$, $w^1(\zeta,z,\xi)$, $T_1^2(\zeta,z,\xi)$, $T_2^0(\zeta,z,\xi)$ and $\sigma_z^1(\zeta,z,\xi)$, respectively, which are given by Ai (1999).

If the unknown quantities at the depth z in the i^{th} layer are above the loading level in which the horizontal circular load is applied, as shown in **Fig. 2**, $\tilde{\Psi}(\zeta,z,\xi)$ can be derived from

$$\tilde{\Psi}(\zeta,z,\xi) = \Phi(\zeta,z-H_{i-1})\Phi(\zeta,H_{n-1})L\Phi(\zeta,\Delta H_1)\tilde{\Psi}(\zeta,0,\xi) \quad (H_{i-1} < z \le H_i, z \le H_{m1}) \qquad [21]$$

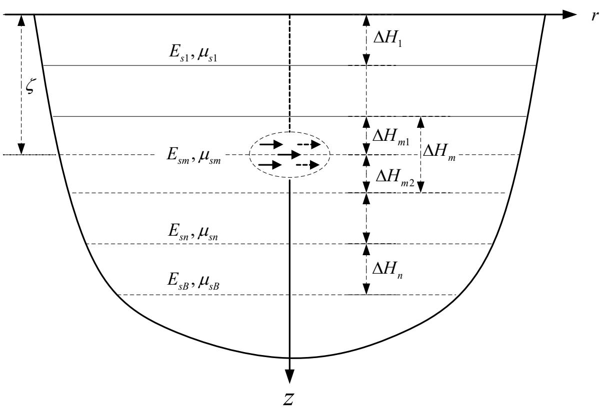

Fig. 2. Horizontal circular load in elastic layered soils.

where $\Phi(\zeta,z)=$ 6×6 size transfer matrix. It can be written as

$$\Phi_{11}=\frac{\zeta z\times sh\zeta z}{4(1-\mu)}+ch\zeta z=\Phi_{22}=\Phi_{44}=\Phi_{55}$$

$$\Phi_{12}=-\frac{\zeta z\times sh\zeta z}{4(1-\mu)}=\Phi_{21}=\Phi_{45}=\Phi_{54}$$

$$\Phi_{13}=\frac{\zeta z\times ch\zeta z}{2(1-\mu)}+\frac{(1-2\mu)sh\zeta z}{2(1-\mu)}=-\Phi_{23}=-2\Phi_{64}=2\Phi_{65}$$

$$\Phi_{14}=\frac{z\times ch\zeta z}{8G(1-\mu)}+\frac{(7-8\mu)sh\zeta z}{8G(1-\mu)\zeta}=\Phi_{25}$$

$$\Phi_{15}=-\frac{z\times ch\zeta z}{8G(1-\mu)}+\frac{sh\zeta z}{8G(1-\mu)\zeta}=\Phi_{24}$$

$$\Phi_{16}=\frac{z\times sh\zeta z}{4G(1-\mu)}=-\Phi_{26}=-2\Phi_{34}=2\Phi_{35}$$

$$\Phi_{31}=-\frac{\zeta z\times ch\zeta z}{4(1-\mu)}+\frac{(1-2\mu)sh\zeta z}{4(1-\mu)}=-\Phi_{32}=-\frac{1}{2}\Phi_{46}=\frac{1}{2}\Phi_{56}$$

$$\Phi_{33}=-\frac{\zeta z\times sh\zeta z}{2(1-\mu)}+ch\zeta z=\Phi_{66}$$

$$\Phi_{36}=-\frac{z\times ch\zeta z}{4G(1-\mu)}+\frac{(3-4\mu)sh\zeta z}{4G(1-\mu)\zeta}$$

$$\Phi_{41}=\frac{G\zeta^2 z\times ch\zeta z}{2(1-\mu)}+\frac{G(2-\mu)\zeta\times sh\zeta z}{2(1-\mu)}=\Phi_{52}$$

$$\Phi_{42}=-\frac{G\zeta^2 z\times ch\zeta z}{2(1-\mu)}-\frac{G\mu\zeta\times sh\zeta z}{2(1-\mu)}=\Phi_{51}$$

$$\Phi_{43}=\frac{G\zeta^2 z\times sh\zeta z}{1-\mu}=-\Phi_{53}=-2\Phi_{61}=2\Phi_{62}$$

$$\Phi_{63}=-\frac{G\zeta^2 z\times ch\zeta z}{1-\mu}+\frac{G\zeta\times sh\zeta z}{1-\mu}$$

$\tilde{\Psi}(\zeta,0,\xi)$ can be determined from the following transfer matrix

$$\begin{aligned}\tilde{\Psi}(\zeta,0,\xi)=&\Phi(\zeta,-\Delta H_1)\Phi(\zeta,-\Delta H_2)\\&L\Phi(\zeta,-\Delta H_{n-1})\Phi(\zeta,-\Delta H_n)\tilde{\Psi}(\zeta,H_n^+)\\&-\Phi(\zeta,-\Delta H_1)\Phi(\zeta,-\Delta H_2)\\&L\Phi(\zeta,H_{m-1}-\xi)\left[0,0,0,0,\tilde{P},0\right]^T\end{aligned}\qquad[22]$$

where $\tilde{P}$ is the Hankel transform of Eq. [10]

$$\tilde{P}=\sin a\zeta/(2a\pi\zeta)\qquad[23]$$

If the unknown quantities at the depth z in the i^{th} layer is below the loading level, $\tilde{\Psi}(\zeta,z,\xi)$ can be derived from

$$\begin{aligned}\tilde{\Psi}(\zeta,z,\xi)=&\Phi(\zeta,z-H_i)\Phi(\zeta,-H_{i+1})\\&\Phi(\zeta,-\Delta H_n)\tilde{\Psi}(\zeta,H_n^+)\ (H_{i-1}<z<H_i,z>H_{m1})\end{aligned}\qquad[24]$$

$\tilde{\Psi}(\zeta,H_n^+)$ is expressed as

$$\begin{aligned}\tilde{\Psi}(\zeta,H_n^+)=&\Phi(\zeta,\Delta H_n)\Phi(\zeta,\Delta H_{n-1})\\&\cdots\Phi(\zeta,\Delta H_{m2})\Phi(\zeta,\xi-H_{m-1})\\&\cdots\Phi(\zeta,\Delta H_1)\tilde{\Psi}(\zeta,0)+\Phi(\zeta,\Delta H_n)\\&\cdots\Phi(\zeta,\Delta H_{m2})\left[0,0,0,0,\tilde{P},0\right]^T\\&(H_{i-1}<z<H_i,z>H_{m1})\end{aligned}\qquad[25]$$

4. Illustrative results and discussion

4.1 Comparison of the proposed analysis with other existent solutions

Based on the strain-potential approach proposed by Muki (1960) for asymmetric problem in the theory of elastic, the displacement influence function has been obtained by Pak (1989). In this study, the normalized displacement influence function is determined using the transfer matrix method. To confirm the validity of the proposed solution, the present solutions using the transfer matrix method for the laterally loaded piles in layered soils will be compared to with a nondimensional solution obtained by Pak (1989) for the piles in homogeneous elastic soil.

The model of the laterally loaded piles in three-layer soils is shown in **Fig. 3 (b)**. In the three-layer soil analyses, the writers have assumed that $\Delta H_1=0.3L$ and $\Delta H_2=0.7L$ respectively for the thickness of the upper soil layers, $\mu_{s1}=\mu_{s2}=0.3$ for the Poisson's ratios, and $E_p/E_{s2}=E_p/E_{s1}=E_p/E_{sB}=\bar{E}=1000,5000$ for the ratios of the layered soil stiffness. As shown in **Fig. 4**, the bending moment, slope and displacement distributions from the two methods are in good agreement, which confirms the validity of the present formulation and numerical scheme.

4.2 Parametrical studies

The influences of some parameters and soil layering on the calculated bending moment, slope and displacement of laterally loaded piles in two-layer soils and three-layer soils are studied in detail in this section. The model of the laterally loaded piles in two-layer soils and three-layer soils are shown in **Fig. 3** for the ratio of the base stiffness to the top soil stiffness $E_{sB}/E_{s1}=10$, pile slenderness ratio of $L/a=60$, the base soil Poisson's ratio of $\mu_{sB}=0.3$ and pile-soil stiffness ratios of $E_p/E_{s1}=100, 1000$, and 5000. In the three-layer soil analyses, the writers have assumed that $\Delta H_1=0.4L$ and $\Delta H_2=0.6L$ respectively for the thickness of the upper soil layers, $\mu_{s1}=\mu_{s2}=0.3$ for the Poisson's ratios, and $E_{s2}/E_{s1}=4$ for the ratio of the layered soil stiffness. As shown in **Fig. 3 (b)**, the thickness of the upper two-layer soils is L.

Figs. 5 and **6** illustrate solutions for shear loading only and moment loading only, respectively. It can be observed that for both layered soil systems there is a poor agreement of the variation of bending moment, slope and displacement along the direction of normalized depth. With the increase of the normalized depth $\bar{z}$, the bending moment, slope and displacement profiles under both shear and moment loading cases in three-layer soils tend to have a more apparent reversal at some depth. This feature reflects that the lateral loads applied to the pile are transferred to a great depth in three-layer soils. The examples show that explicit accounting of the different layers is necessary for accurate prediction of the laterally loaded pile response.

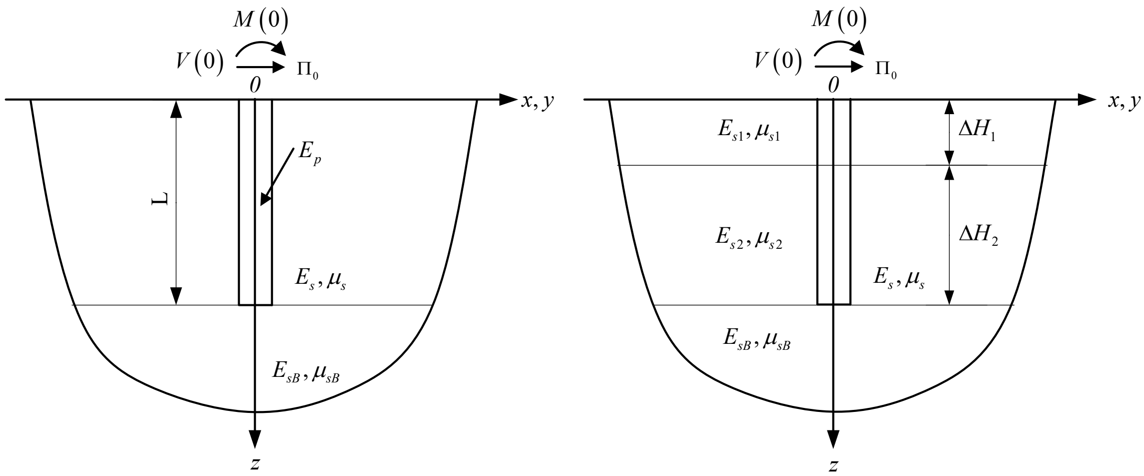

(a) Two-layer soils (b) Three-layer soils

Fig. 3. Model of laterally loaded pile in layered soils.

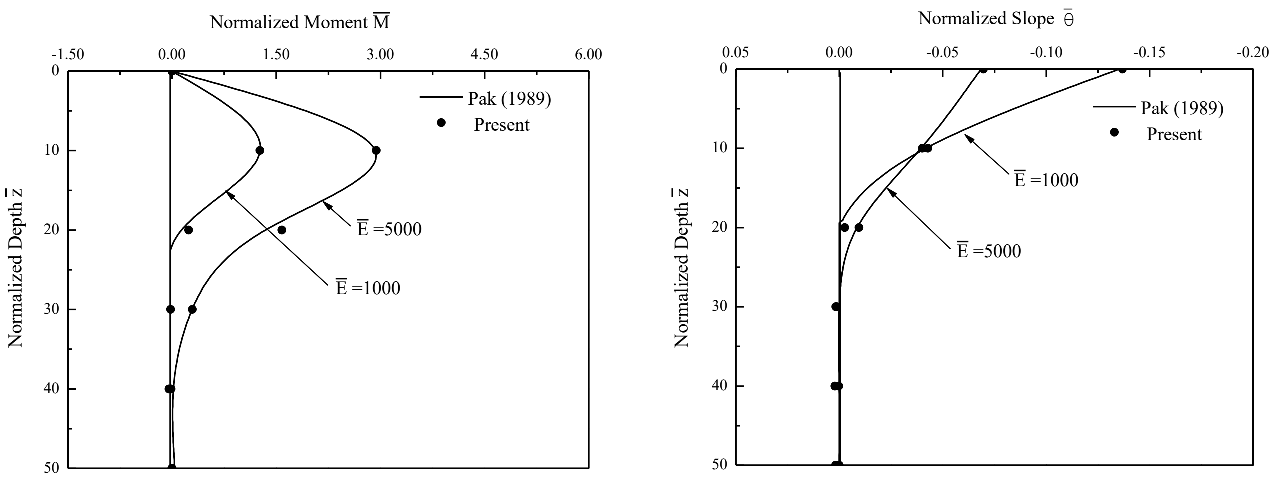

(a) Bending moment profile (b) Slope profile

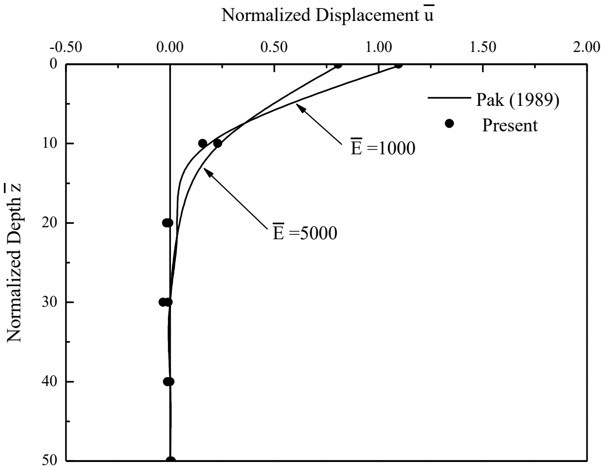

(c) Displacement profile

Fig. 4. Bending moment, slope and displacement distributions under unit shear.

The normalized slope for the two layered soil systems and loading conditions are shown in **Figs. 5(c, d)** and **Figs. 6(c, d)**, while the corresponding normalized displacement are illustrated in **Figs. 5(e, f)** and **Figs. 6(e, f)**, respectively. In accord with the reciprocal theorem in linear elastostatics, the absolute value of the top rotation due to a unit shear is found to be identical to the top displacement due to a unit moment for the whole range of modulus ratios and both layered soil systems.

5. Conclusions

This paper is aimed at establishing a rigorous method of analysis for a single, circular pile embedded in multi-layered soils and subjected to a horizontal force and a moment at the pile top. The main findings and conclusions from this study are as follows:

(1) A fictitious-pile expression for estimating the pile-soil interaction in multi-layered soils was established, which was formulated as a Fredholm integral equation of the second kind. The validity of the current method has been verified through comparisons with existing solutions.

(2) In particular, it has been shown that soil layering has a definite impact on the pile response. Hence, proper accounting of the soil layers is necessary to accurately predict the lateral pile response. The new fictitious-pile expression and the theory of the transfer matrix for the laterally loaded pile have the capability of predicting the pile response with full consideration of soil layering.

(3) For the whole range of modulus ratios and both layered soil systems, the absolute value of the top rotation due to a unit shear is found to be identical to the top displacement due to a unit moment.

Acknowledgements

Financial supports from the Innovation Project of Shanghai Education Committee (NO. 15ZZ103) and the Key Science research of Shanghai Open University (NO. JF1301) are gratefully acknowledged.

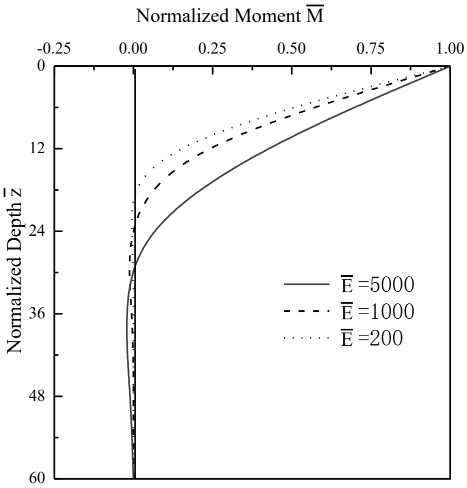

(a) Bending moment profile in two-layer soils

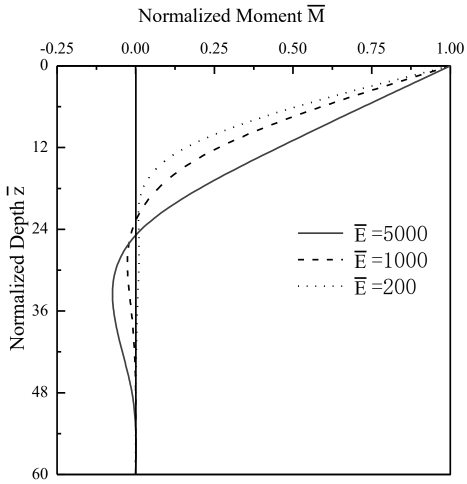

(b) Bending moment profile in three-layer soils

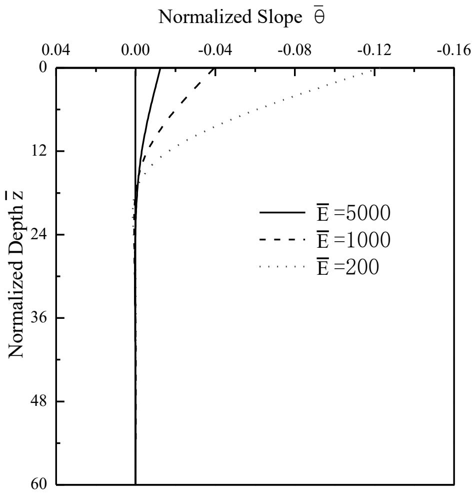

(c) Slope profile in two-layer soils

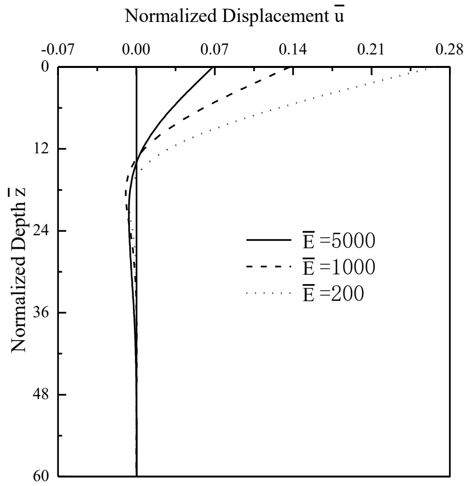

(e) Displacement profile in two-layer soils

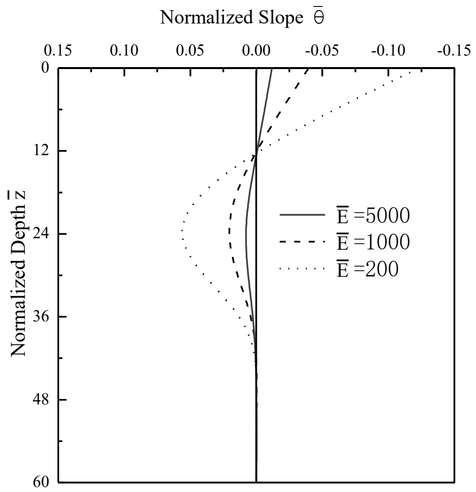

(d) Slope profile in three-layer soils

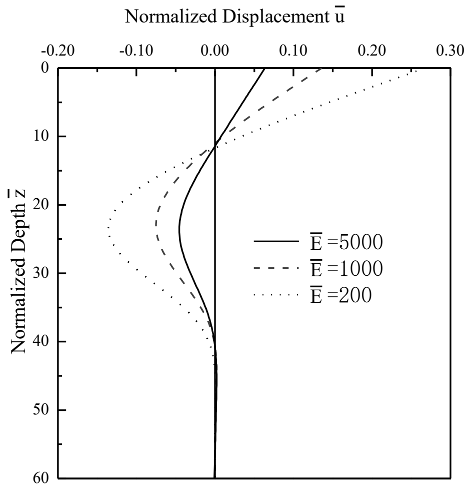

(f) Displacement profile in three-layer soils

Fig. 5. Bending moment, slope and displacement distributions under unit moment.

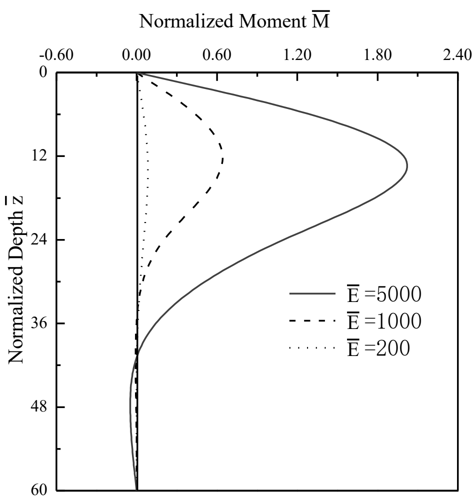

(a) Bending moment profile in two-layer soils

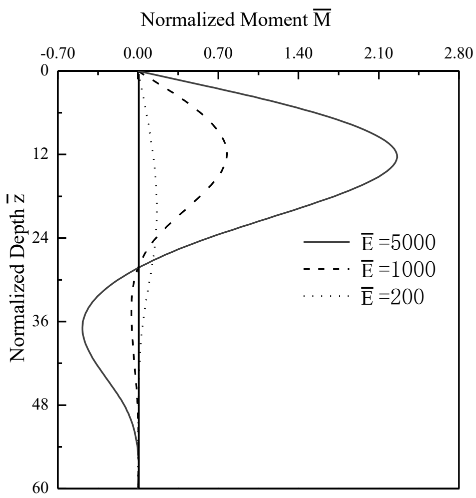

(b) Bending moment profile in three-layer soils

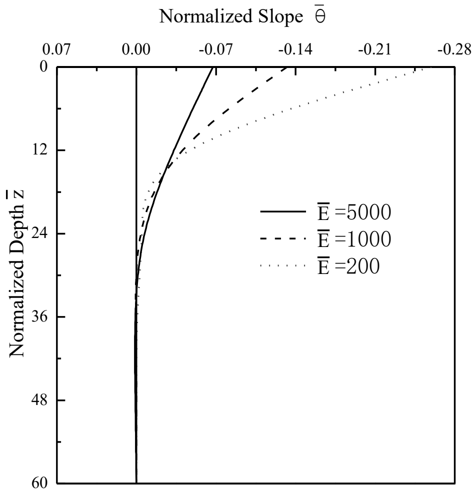

(c) Slope profile in two-layer soils

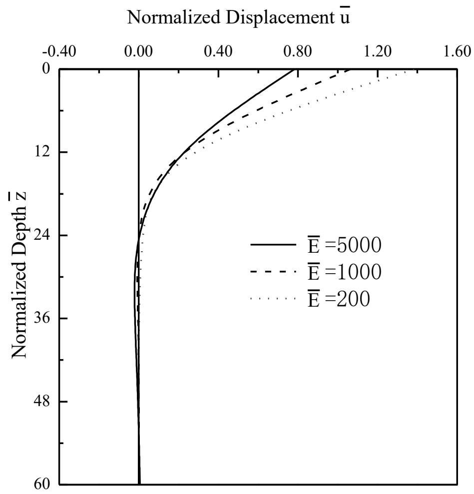

(e) Displacement profile in two-layer soils

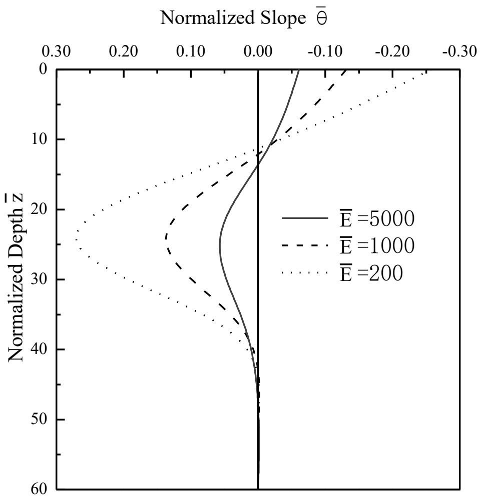

(d) Slope profile in three-layer soils

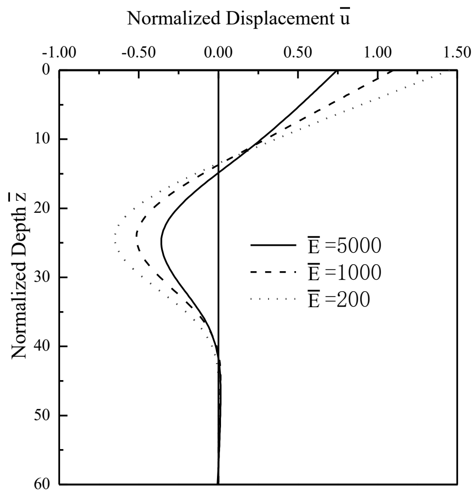

(f) Displacement profile in three-layer soils

Fig. 6. Bending moment, slope and displacement distributions under unit shear.

References

Ai, Z.Y., 1999. Research on theory of layered elastic system and its application in piled raft foundation. PHD dissertation, Tongji University, Shanghai, China.

Ai, Z.Y., Yue, Z.Q., Tham, L.G. and Yang, M., 2002. Extended Sneddon and Muki solutions for multilayered elastic materials. International Journal of Engineering Science, **40**: 1453-1483.

Bahar, L.Y., 1972. Transfer matrix approach to layered systems. Journal of Engineering Mechanics Division, ASCE, **98**: 1159-1172.

Banerjee, P.K. and Davis, T.G., 1978. The behavior of axially and laterally loaded single piles embedded in non-homogeneous soils. Geotechnique, **28** (3): 309-326.

Basu, D., Salgado, R., 2007. Elastic analysis of laterally loaded pile in multi-layered soil. J. Geomechanics and Geoengineering, **2** (3): 183-196.

Basu, D., Salgado, R., 2010. Analysis of laterally loaded piles with rectangular cross sections embedded in layered soil. International Journal for Numerical and Analytical Methods in Geomechanics, **32** (7): 721-744.

Basu, D., Salgado, R. and Prezzi, M., 2009. A continuum-based model for analysis of laterally loaded piles in layered soils. Geotechnique, **59** (2): 127-140.

Bufler, H., 1971. Theory of elasticity of a multi-layered medium. Journal of Elasticity: 125-143.

Cao, M., 2017. Fictitious pile approach and parametric analysis of laterally loaded piles. Journal of Civil, Architectural and Environmental Engineering, **39** (3): 115-121.

Cao, M. and Chen, L.Z., 2008. Analysis of interaction factors between two piles. Journal of Shanghai Jiaotong University(Sci), **13** (2): 171-176.

Cao, M. and Chen, L.Z., 2011. Analysis of interaction factors between two piles in layered soils. Journal of Donghua University, **28** (3): 255-260.

Cao, M., Chen, L.Z., Chen, S.L.,2007. An innovative approach to evaluate the behaviour of vertically loaded pile groups based on elastic theory. Lowland Technology International, **9** (1): 1-10.

Cao, M. and Chen, S.L., 2012. An elastic theory approach and parametric analysis of pile group in layered soils. Journal of Civil, Architectural and Environmental Engineering, **34** (2): 1-6.

Davisson, M.T. and Gill, H.L., 1963. Laterally loaded piles in a layered soil system. J Soil Mech and Found Div, **89** (3): 63-94.

Hetenyi, M., 1946. Beams on elastic foundations. University of Michigan Press, Ann Arbor, Mich.

Matlock, H., 1970. Correlations for design of laterally loaded piles in soft clay. Proc 2nd Offshore Technology Conf, Houston: 577-594.

Mindlin, R.D., 1936. Force at a point in the interior of semi-infinite solid. Physics, **7**: 195-202.

Muki, R., 1960. Asymmetric problems of the theory of elasticity for a semi-infinite solid and a thick plate. Progress in Solid Mech, **6**: 401-439.

Muki, R. and Sternberg, E., 1968. On the diffusion of load from a transverse tension bar into a semi-infinite elastic sheet. Journal of Applied Mechanics, **35**: 737-746.

Muki, R. and Sternberg, E., 1970. Elastostatic load-transfer to a half-space from a partially embedded axially loaded rod. International Journal of Solids and Structures, **6**: 69-90.

Ng, C.W.W. and Zhang, L.M., 2001. Three-dimensional analysis of performance of laterally loaded sleeved piles in sloping ground. Journal of Geotechnical and Geoenvironmental Engineering, **127** (6): 499-509.

Pak, R.Y.S., 1989. On the flexure of a partially embedded bar under lateral loads. Journal of Applied Mechanics Division, ASME, **56**: 263-269.

Pise, P.J., 1982. Laterally loaded piles in a two-layer soil system. Journal of the Geotechnical Engineering, ASCE, **108** (9): 1177-1181.

Poulos, H.G., 1971. Behavior of laterally loaded piles: I-Single piles. J Soil Mech and Found Div, 97(5): 711-731.

Poulos, H.G. and Davis E.H., 1980. Pile foundation analysis and design. Wiley.

Randolph, M.F., 1981. The response of flexible piles to lateral loading. Geotechnique, **31** (2): 247-259.

Reese, L.C. and Matlock, H., 1956. Non-dimensional solutions for laterally loaded piles with soil modulus assumed proportional to depth. Proc. 8th Texas Conf on Soil Mechanics and Foundation Engineering, Austin, Tex, 1-23.

Reese, L.C., Cox, W.R. and Koop, F.D., 1974. Analysis of laterally loaded pile in sand. In: Proc. 6th Annual Offshore Technology Conference, Houston (TX). Paper no. 2080.

Reese, L.C. and Welch, R.C., 1975. Lateral loading of deep foundations in stiff clay. J Geotech Engrg Div, **101** (7): 633-649.

Shen, S.L. and Xu, Y.S., 2011. Numerical evaluation of land subsidence induced by groundwater pumping in Shanghai. Canadian Geotechnical Journal, **48** (9): 1378-1392.

Shen, S.L., Ma, L., Xu, Y.S. and Yin, Z.Y., 2013a. Interpretation of increased deformation rate in aquifer IV due to groundwater pumping in Shanghai. Canadian Geotechnical Journal, **50** (11): 1129-1142.

Shen, S.L., Wang, Z.F., Yang, J. and Ho, E.C., 2013b. Generalized approach for prediction of jet grout column diameter. Journal of Geotechnical and Geoenvironmental Engineering, **139** (12): 2060-2069.

Shen, S.L., Wang, Z.F., Horpibulsuk, S. and Kim, Y.H., 2013c. Jet-Grouting with a newly developed technology: the Twin-Jet Method. Engineering Geology, **152** (1), 87-95.

Shen, S.L., Wang, Z.F., Sun, W.J., Wang, L.B. and Horpibulsuk, S., 2013d. A field trial of horizontal jet grouting using the composite-pipe method in the soft deposit of Shanghai. Tunneling and Underground Space Technology, **35**: 142-151.

Shen, S.L., Wu, H.N., Cui, Y.J. and Yin, Z.Y., 2014. Long-term settlement behavior of the metro tunnel in Shanghai. Tunneling and Underground Space Technology, **40**: 309-323.

Shen, S.L., Cui, Q.L., Ho, E.C. and Xu, Y.S., 2016. Ground response to multiple parallel microtunneling operations in cemented silty clay and sand. Journal of Geotechnical and Geoenvironmental Engineering, **142** (5): 04016001(1-11).

Shen, S.L., Wang, Z.F. and Cheng, W.C., 2017. Estimation of lateral displacement induced by jet grouting in clayey soils. Geotechnique, ICE, (DOI): 10.1680/geot./16-P-159.

Sneddon, I.N., 1992. On Muki's solution of the equations of linear elasticity. Intl. J. Eng Sci, **30** (10): 1237-1246.

Trochanis, A.M., Bielak, J. and Christiano, P., 1991. Three-dimensional nonlinear study of piles. J. Geotech Engrg., **117** (3): 429-447.

Wang, Z.F., Shen, S.L., Ho, E.C. and Kim, Y.H., 2013. Investigation of field installation effects of horizontal Twin-Jet grouting in Shanghai soft soil deposits. Canadian Geotechnical Journal, **50** (3): 288–297.

Wang, Z.F., Shen, S.L., Ho, C.E. and Xu, Y.S., 2014. Jet grouting for mitigation of installation disturbance. Geotechnical Engineering, ICE Proceedings, **167** (GE6), 526-536.

Wu, H.N., Shen, S.L., Liao, S.M. and Yin, Z.Y., 2015a. Longitudinal structural modelling of shield tunnels considering shearing dislocation between segmental rings. Tunneling and Underground Space Technology, **50**: 317-323.

Wu, Y.X., Shen, S.L., Xu, Y.S. and Yin, Z.Y., 2015b. Characteristics of groundwater seepage with cutoff wall in gravel aquifer. I: Field observations. Canadian Geotechnical Journal, **52** (10): 1526-1538.

Wu, Y.X., Shen, S.L., Yin, Z.Y. and Xu, Y.S., 2015c. Characteristics of groundwater seepage with cutoff wall in gravel aquifer. II: Numerical analysis. Canadian Geotechnical Journal, **52** (10): 1539-1549.

Wu, Y.X., Shen, S.L., Wu, H.N., Xu, Y.S. Yin, Z.Y. and Sun, W.J., 2015d. Environmental protection using dewatering technology in a deep confined aquifer beneath a shallow aquifer. Engineering Geology, **196**: 59-70.

Wu, Y.X., Shen, S.L. and Yuan, D.J., 2016. Characteristics of dewatering induced drawdown curve under barrier effect of retaining wall in aquifer. Journal of Hydrology, **539**: 554-566.

Xu, Y.S., Shen, S.L., Ren, D.J. and Wu, H.N., 2016. Analysis of factors in land subsidence in Shanghai: a view based on a strategic environmental assessment. Sustainability, **8** (6): pp 573.

Yang, C.C., Lin, S.S., Juang, C.H. and Wei F.L., 2002. Analysis of laterally loaded piles in a two-layered elastic medium. Deep Foundations, **116**: 80-94.

Yang, K. and Liang, R., 2006. Numerical solution for laterally loaded piles in a two-layered soil profile. Journal of Geotechnical and Geoenvironmental Engineering, ASCE, **132** (11): 1436-1443.

Zhang, N., Shen, S.L, Wu, H.N., Chai, J.C. and Yin, Z.Y., 2015. Evaluation of performance of embankments with reinforcement on PVD-improved marine clay. Geotextiles and Geomembranes, **43** (6): 506-514.